



# Lab on a Chip

## Ultra-simple Wearable Local Sweat Volume Monitoring Patch Based on Swellable Hydrogels

Journal:	<i>Lab on a Chip</i>
Manuscript ID	LC-ART-09-2019-000911.R1
Article Type:	Paper
Date Submitted by the Author:	01-Nov-2019
Complete List of Authors:	Zhao, Feijun; Guilin University of Electronic Technology, Key Laboratory of Biomedical Sensing and Intelligent Instruments; University of Cincinnati, Novel Device Lab Bonmarin, Mathias; Zurcher Hochschule fur Angewandte Wissenschaften, CP Institute of Computational Physics Chen, Zhencheng; Guilin University of Electronic Technology, Key Laboratory of Biomedical Sensing and Intelligent Instruments Larson, Mikel; Eccrine Systems Inc Fay, Dan; Eccrine Systems Inc Runnoe, David; Eccrine Systems Inc Heikenfeld, Jason; University of Cincinnati, Novel Device Lab

SCHOLARONE™  
Manuscripts



## Ultra-simple Wearable Local Sweat Volume Monitoring Patch Based on Swellable Hydrogels

F. J. Zhao<sup>a, b</sup>, M. Bonmarin<sup>b, c</sup>, Z. C. Chen<sup>a\*</sup>, M. Larson<sup>d</sup>, D. Fay<sup>d</sup>, D. Runnoe<sup>d</sup>, and J. Heikenfeld<sup>b\*</sup>

Received 00th January 20xx,  
Accepted 00th January 20xx

DOI: 10.1039/x0xx00000x

[www.rsc.org/](http://www.rsc.org/)

Quantifiably monitoring sweat rate and volume is important to assess the stress level of individuals and/or prevent dehydration, but despite intense research, a convenient, continuous, and low-cost method to monitor sweat rate and total sweat volume loss remains an un-met need. We present here an ultra-simple wearable sensor capable of measuring sweat rate and volume accurately. The device continuously monitors sweat rate by wicking the produced sweat into hydrogels that measurably swell in their physical geometry. The device has been designed as a simple to fabricate, low-cost, disposable patch. This patch exhibits stable and predictable operation over the maximum variable chemistry expected for sweat (pH 4-9 and salinity 0-100 mM NaCl). Preliminary *in vivo* testing of the patch has been achieved during aerobic exercise, and the sweat rates measured via the patch accurately follow actual sweat rates.

### Introduction

Eccrine sweat has recently gained significant attention as a non-invasive biofluid for continuous measurement of blood analytes.<sup>1,2</sup> The majority of research has focused on implementing chemical sensors in wearable patches, with a recent report demonstrating for the first time complete *in vivo* validation of continuous sweat data that correlates with blood data.<sup>3</sup> In addition, there are two known physiological conditions that can be continuously measured in sweat *without* chemical sensors: (1) decades-old use of galvanic skin response as a non-quantitative measure of mental or physical stress;<sup>4</sup> (2) total sweat volume loss, which can be used to predict and prevent dehydration. The latter, dehydration, has a very large impact spanning wellness, sport, workforce, and medicine, but has been relegated to inconvenient measures such as nude body weight.<sup>5</sup> A convenient, continuous, and low-cost method to monitor sweat rate and total sweat volume loss is, therefore, a significant un-met need. Although this application may sound like it should be simple to serve with wearable technology, no demonstration to date has fully addressed the complete set of challenges and ideal requirements (see Requirements and Challenges). Presented here is a novel wearable patch that is able to continuously

monitor total sweat volume and therefore sweat rate, by wicking of sweat into hydrogels that measurably swell in their physical geometry (Fig. 1). Importantly, the patch is designed such that when it is on the body the only stimulus that can cause the hydrogels to swell is absorption of sweat as it is wicked up off the skin surface. The patch contains a custom-synthesized super absorbent material that is cut into hexagons or grids which increase in visible surface area up to ~2X with absorption of sweat. The patch is optimized for typical high sweat generation rates of 100's-1000's of nL/cm<sup>2</sup>.<sup>6</sup> Importantly, the patch is not confounded by changing pH (4-9) and salinity (0-100 mM), both of which are highly variable in sweat<sup>2,6</sup>. Also demonstrated are two modes of operation: (1) geometry change recorded by a smart-phone camera (Fig. 1c); (2) optical reflectance that can be continuously monitored without requiring any user-action (Fig. 1d). *In vivo* demonstration also matches the *in vitro* predicted performance. These results confirm the potential to meet the unmet need for continuously measuring sweat volume loss and sweat rate with simple and low-cost wearable patches.

### Requirements and Challenges

In our own earliest work we pursued wearable patches to measure sweat generation rate and electrolyte loss using methods such as galvanic skin response and ion-selective electrodes.<sup>7</sup> We quickly abandoned these early efforts as our understanding improved on the primary value such a device would provide, and on the real challenges that exist for such a device. In terms of value, we currently speculate that in most use-cases, reliably measuring body water volume loss due to sweating is the single most important measure, and that other measures such as real time sweat rate or electrolyte concentrations are less valuable in preventing bodily

<sup>a</sup> College of Electronic Engineering and Automation, Guilin University of Electronic Technology, Guilin, Guangxi 541004, China.

<sup>b</sup> Novel Devices Laboratory, University of Cincinnati, Cincinnati, Ohio 45221, USA.

<sup>c</sup> School of Engineering, Zurich University of Applied Sciences, Technikumstrasse 9, Winterthur, Zurich 8400, Switzerland.

<sup>d</sup> Eccrine Systems Inc., 1775 Mentor Ave, Cincinnati, Ohio 45212, USA.

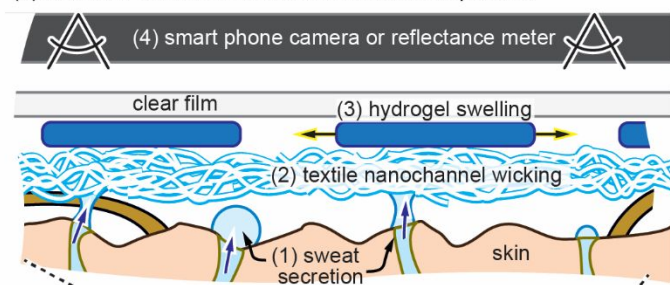
\*Corresponding Author

Electronic Supplementary Information (ESI) available: AutoCAD Device Layout, Additional Data.

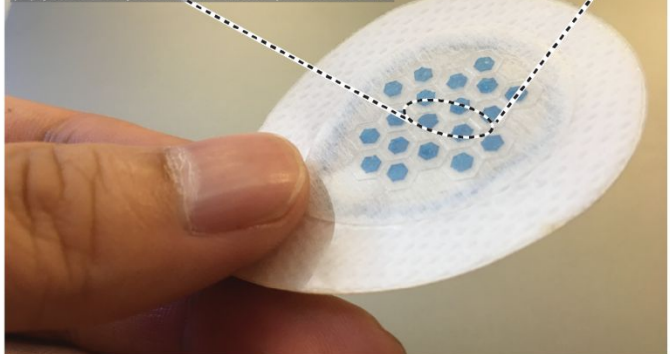
## ARTICLE

Journal Name

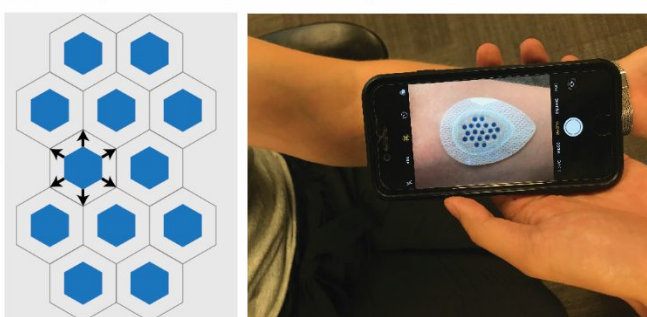
(a) side view of basic device construction and operation



(b) photo of patch for smart-phone mode



(c) smart-phone mode (measure hexagon area)



(d) smart-watch mode (measure decreasing optical reflectance)



**Fig. 1** Wearable sweat volume monitoring patch: (a) side view of basic device construction and operation. A textile nanochannel wicking material is placed in contact with the skin. The sweat secretion collected by the textile comes in contact with a swellable hydrogel film which increases in volumes as sweat is absorbed. Two geometrical configurations were developed where: (b,c) the hydrogel area can be imaged and quantified; or (d) where the patch reflectance can be optically measured. In the smart-phone mode (c) hexagonal pieces of hydrogel extend their surface area whereas in the smart-watch mode (d) the white uncovered textile surface area decreases with sweat absorption leading to a decrease of the optical reflectance.

dehydration.<sup>1,2</sup> Our rationale is two-fold. Firstly, if you can predict bodily fluid volume loss then you can predict when to ingest fluids, which in most cases will also adequately replenish electrolytes if something as simple as a sports-drink is utilized. Simply, knowing when to rehydrate generally resolves both bodily hydration and electrolyte balance. Secondly, and most importantly, reliably predicting bodily water volume loss due to sweating is very difficult. Bodily sweat rate varies significantly from individual to individual, changes with degree of fitness<sup>8</sup>, and depends on activity level and environment. Furthermore, from literature data it appears that for some of the general population, the maximum bodily sweat rate can even exceed the rate at which an individual is able to re-absorb water through the gut (ingestion).<sup>9–11</sup>

With an application-focus now placed on accurately measuring total body sweat volume loss, requirements and challenges from a *device* perspective can now be discussed with greater clarity. In terms of major device requirements, because sweat is a biofluid it is challenging to envision a device that would work reliably beyond a single usage without extra work by the user (drying, cleaning, etc). Therefore, it is likely that a device will require a disposable component that includes both sweat collection and transducing the collected sweat volume into a measurable signal. Such a disposable component can then be combined with a reusable component that electrically or optically measures that signal (Fig. 1c, 1d). From a cost perspective, an ideal disposable component would therefore be free from features such as sensors or electronics. This motivated the design of the ultra-simple disposable patch

shown in Fig. 1, which includes only adhesives, textiles, hydrogel, and a clear cover material.

The on-body environment presents several significant challenges that also guided patch design in this work. These challenges are not so severe that they form strict requirements, but if not addressed they will reduce measurement accuracy. To the best of our knowledge, these challenges have not yet been directly addressed in previous literature.<sup>2,12–17</sup> A first challenge is that pH and salinity of sweat changes significantly with sweat rate and across individuals. Variable salinity (10–100 mM) can confound accuracy in electrical conductance measurements of sweat volume as it fills a channel.<sup>15,16</sup> A second challenge is body-motion and muscle contraction induced flow-reversal of a sweat volume collected in a channel that is sealed against the skin-surface. This can impact position-based sensing of sweat in a channel or potential-use of in-line flow meters to measure velocity of flow of sweat in a channel.<sup>17</sup> A third challenge arises when using an adhesive seal and the positive pressure created by sweat generation to push sweat into a channel. Adhesives and positive-pressure flow may be feasible for stimulated sweat,<sup>13</sup> but is likely very challenging for natural sweating because sweat that emerges beneath the adhesive may either move into the channel or to the outside edge of the patch (i.e. sweat collection area is uncontrolled).<sup>14</sup> This is an important challenge that has not been discussed in any previous work, despite it having a potentially strong negative impact on measurement accuracy. A fourth challenge is that sweat rate is highly variable across the body,<sup>15</sup> therefore whatever device is

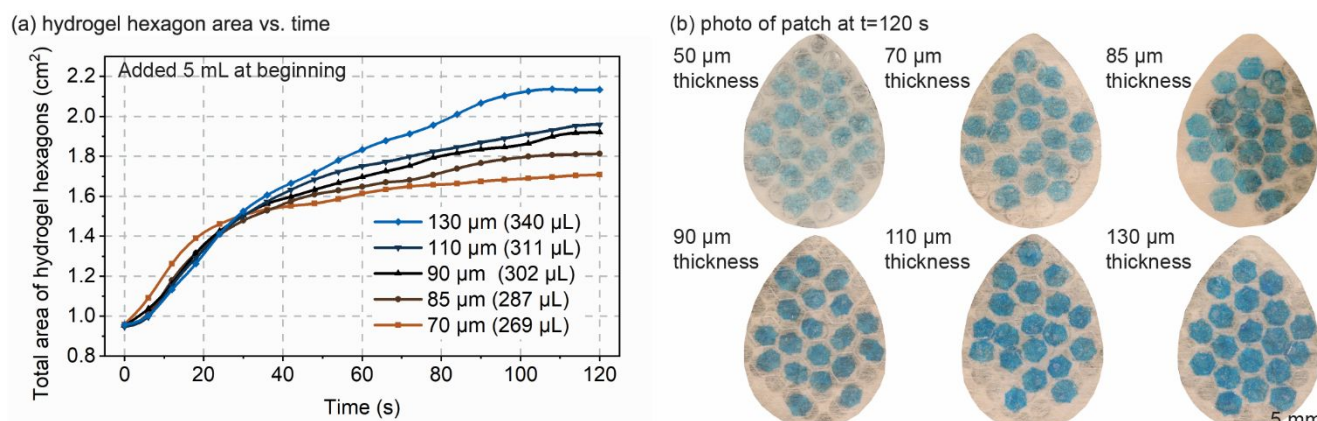


**Fig. 2** Influence of the hydrogel thickness. (a) Total combined visible area of the 19 hydrogel hexagons in each patch vs. time after 5 mL of 1 mM NaCl solution was added all at once to the patch. This fluid volume exceeds the total fluid capacity of the patch, such that measurements could be made of the maximum rate of swelling and the maximum swelling capacity. (b) Picture of the different hydrogel thickness in tested patches after they are fully saturated with liquid.

utilized, maximally accurate measure of total sweat volume loss for the entire body could require at least initial calibration of a specific individual in a specific sweating scenario. Such calibration will likely require multiple patches at multiple body locations, as has been recently validated with on-body patches<sup>15</sup>. Only after total-body-calibration can a single or few body locations then be used to represent total body sweat loss.

With the above requirements and challenges in mind, the patch described in this work was specifically designed to: (1) have a disposable component with a low cost arguably similar to that of a band-aid; (2) to measure sweat volume directly (not indirectly such as electrical conductivity) using geometric change in a hydrogel as it swells with sweat; (3) *very importantly*, use a wicking mode device with an additional hydrogel seal ring (Fig. 5a) such that the sweat collection area is well defined; (4) allow the most desirable use case with a continuous wearable sensor (Fig. 1d), but also using smartphone camera mode for lower-profile patches or for inexpensive whole-body calibration with multiple disposable patches.

### Basic Patch Materials and Function

The basic wearable patch (Fig. 1) contains a textile nano-channel wicking layer, a coloured hydrogel that swells, and a clear upper film to prevent evaporation of water and/or contamination of the hydrogel from external water/sweat. The textile wicking layer serves to provide a wicking contact to the entire collection area, and also provides white reflective background to contrast against the coloured hydrogel. Rayon was utilized for the textile wicking layer with 6.80 cm<sup>2</sup> total area, 0.64 mm thickness, and 4.02 cm<sup>2</sup> contact with skin. Rayon was chosen because it wicks sweat along nano-grooves in the Rayon such that the Rayon layer need not become saturated (full of sweat) before it can transport sweat from the skin to the hydrogels. The total fluid volume of the Rayon is therefore at most  $\sim 6\%$  of the thickness of the Rayon

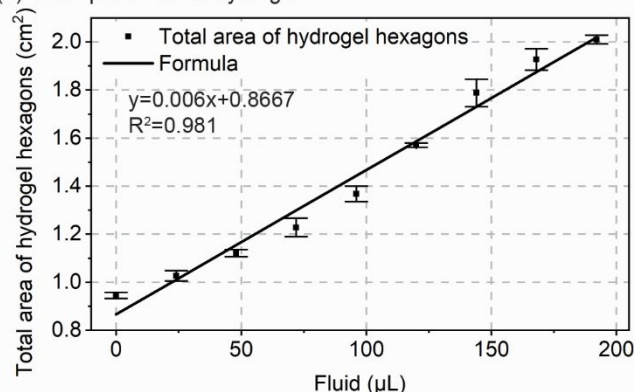
(measured by edge-wicking water into the Rayon and re-weighing it). Use of Rayon was inspired by previous use of sweat sensing patches<sup>18</sup> and is adequate for this work because no analytes in the sweat are being measured (Rayon suffers from analyte exchange).<sup>19</sup> At a thickness of 0.64 mm, the Rayon creates a dead-volume in the patch that is  $\sim 4 \mu\text{L}/\text{cm}^2$  or less. Onto the Rayon, hexagons of blue-coloured hydrogel are placed (see Methods) with geometry of 2.8 mm diameter and 50–130  $\mu\text{m}$  thickness. The hexagons occupy 23.6% of the total Rayon collection area. As the hexagons absorb sweat they increase in geometry, which can then be measured by taking a photo of the hexagon and using software to analyse the increased size (Fig. 1c) or by measuring the decreased optical reflectance of non-blue light as the blue hydrogel covers more area of the white-coloured Rayon (Fig. 1d). The hexagons are also kept separated by a surrounding lattice of double-sided adhesive so they can never overlap each other. The full geometry and layers of the patch, along with CAD drawings, can be found in the online supplementary file for this work.

### In vitro Results: Optimizing the Hydrogel Layer

The thickness of the swellable hydrogel material can be adjusted to the amount of sweat that needs to be absorbed. Thinner hydrogel would allow the device to be more sensitive to smaller volumes of sweat, but if the hydrogel is too thin, then: (1) the device could have limited usage time before the hydrogel reaches its swelling capacity; (2) the hydrogel could be too transparent to optically measure; (3) the hydrogel could become very flimsy (mechanically weak) such that horizontal expansion of the hydrogel could be un-reliable (edge-pinning, friction, wrinkling, etc.). It is important to note, that in this work the hydrogel only occupies  $<25\%$  of the total device area, and the hydrogel can always be made thicker or larger, such that prolonged use of the patch (even  $>24$  hours) should be feasible.

## ARTICLE

(a) smart-phone mode hydrogel



(b) smart-watch mode hydrogel

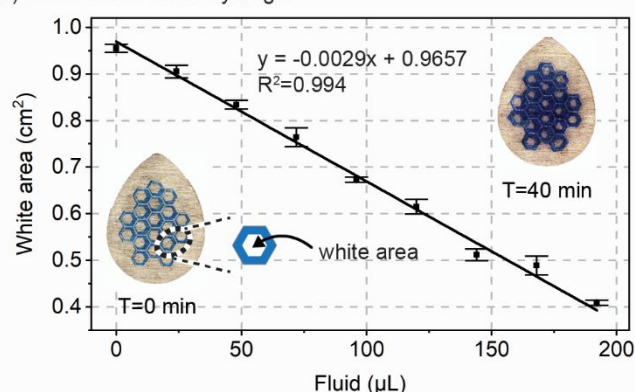


**Fig. 3** Comparison of the smart-phone and smart-watch configuration. (a) Change in total hexagons area vs. fluid uptake using the design shown in Fig. 1c. (b) Decrease of the optical reflectance with fluid uptake using the design shown in Fig. 1d. Very similar behaviour can be observed for both modes. Three separate patches were tested in each data plot (six patches total, all with highly reproducible results).

Fig. 2 demonstrates how varying the initial dry hydrogel thickness (70, 85, 90, 110 and 130 µm) impacts the rate and maximum volume of fluid absorption. The data in Fig. 2 was measured by analyzing the total combined visible area of the 19 hydrogel hexagons in each patch. A hydrogel thickness of 50 µm is not shown in Fig. 2a because at 50 µm thick the hydrogel was too optically transparent and too mechanically flimsy. 5 mL of 1 mM NaCl solution was added all at once to the patch, which exceeds the fluid capacity of the patch, such that measurements could be made of the maximum speed of swelling and the maximum swelling capacity (calculation based on the equation in Fig. 3a). At the beginning, no significant variations can be noticed between the different thicknesses and all hydrogels expand at a similar rate (~0.1–0.2 mm<sup>2</sup>/s) (Fig. 2a). After approximately 40 seconds, the thinner hydrogels tend to quickly plateau in growth rate (0.20 mm<sup>2</sup>/s, 0.31 mm<sup>2</sup>/s, 0.41 mm<sup>2</sup>/s, 0.42 mm<sup>2</sup>/s and 0.60 mm<sup>2</sup>/s for 70, 85, 90, 110 and 130 µm respectively). Hydrogels are known to swell up to 350X–650X of their initial volume,<sup>20</sup> but complete swelling is a longer process (hours or more) and involves weaker swelling force as the hydrogel absorbs more and more water. The maximum swelling of hydrogels was not explored in this work, but as shown in the data of Fig. 2a, was able to swell by 20–30X in volume in less than 2 minutes.

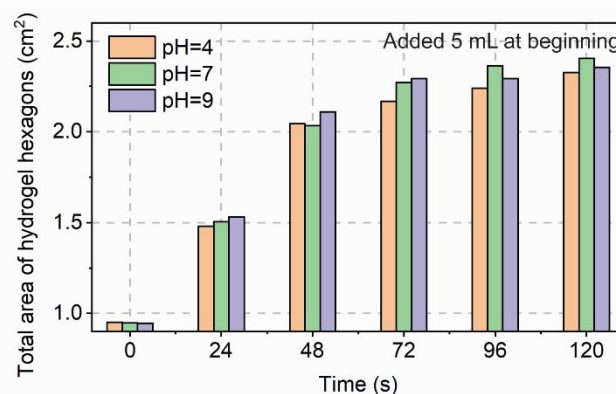
Fig. 2b presents a picture of each patch taken after 120 seconds for different hydrogel thickness. At such a time observable increase in surface area is slowing and/or saturating. As expected, the thicker the material, the larger the surface increase due to improved mechanical strength of the hydrogel film as it expands (less wrinkling). It is visually obvious in Fig. 2b that thinner hydrogels are more geometrically asymmetric, further suggesting that they are mechanically weaker and subject to increased friction/pinning on the Rayon. The colour of the patch is also visibly affected by the hydrogel thickness with the 130 µm sample exhibiting the darkest blue colour. Based on the results of Fig. 2, an 85 µm initial dry hydrogel thickness was chosen for the remainder of the experiments reported here (Figs. 3,4,5).

Next, as shown in Fig. 3a, a calibration curve was created for total combined area of the 19 hydrogel hexagons in each

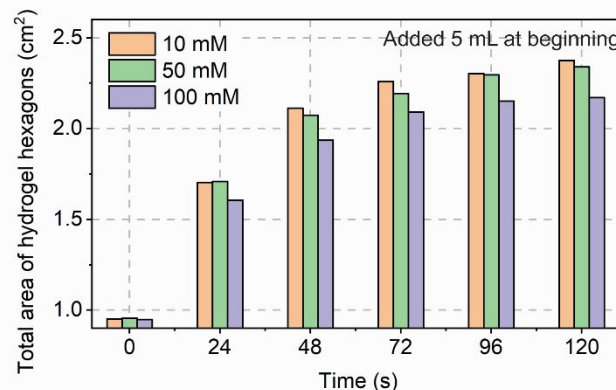
patch vs. volume added. Fluid volume was increased at 4.8 µL/min over 40 minutes for a total final volume of 192 µL. Because the data in Fig. 2 confirmed a rapid swelling response

**Fig. 4** Influence of pH and salinity. (a) pH exhibits little impact on the ability of the hydrogel to expand. (b) increased NaCl concentration tends to decrease the performance of the hydrogel but only significantly at NaCl concentrations that are at the highest end of the physiological range (100 mM). Adjacent bars in the bar-graph all represent a value measured at the same time listed for the x-axis labels.

(a) effects of pH



(b) effects of salinity (NaCl)



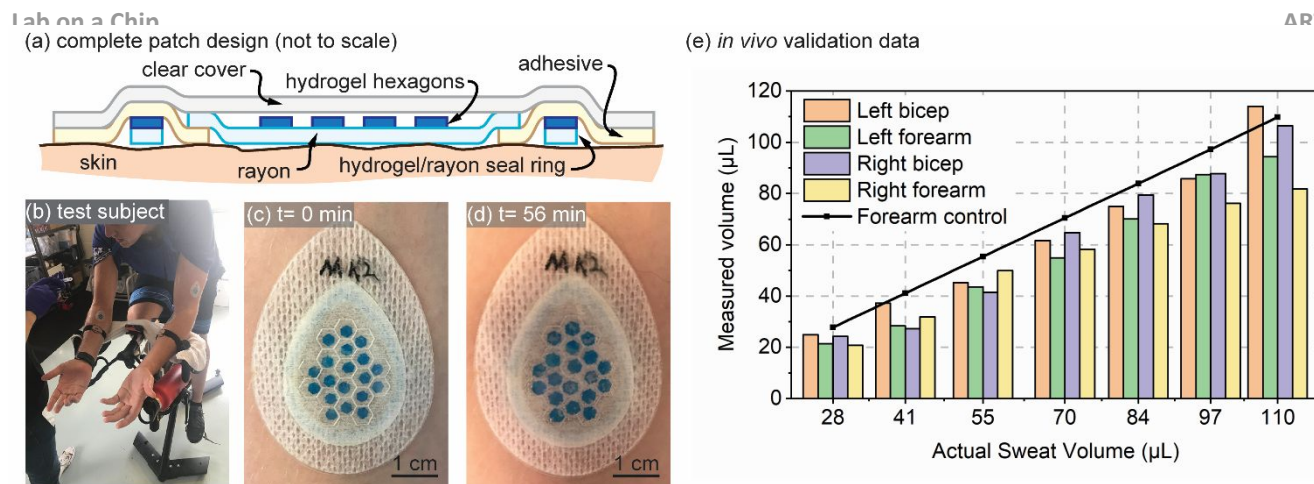


**Fig. 5** *In vivo* validation: (a) full patch design for the *in vivo* testing (not to scale); (b) test-subject setup; (c,d) initial and final photos of an example patch on body; and (e) *in vivo* data for four patches plotted as measured sweat volume vs. actual sweat volume. The actual sweat volume (control) was determined using a separate gravimetric measurement<sup>10</sup>, and the measured sweat is created from patch data using the calibration curve from Fig. 3a. Adjacent bars in the bar-graph all represent a value measured at the same volume listed for the x-axis labels.

for the hydrogels (approximately few minutes), it can be assumed that for each data point in Fig. 3 the hydrogel swelling is complete. For a total sweat collection area of  $\sim 4$  cm<sup>2</sup>, 4.8  $\mu$ L/min would represent a sweat generation rate of  $\sim 1.2$   $\mu$ L/min/cm<sup>2</sup> and for 100 to 150 active glands/cm<sup>2</sup> a glandular sweat generation rate of 12 to 8 nL/min/gland. This confirmed that the smart-phone mode patch design (Fig. 1c) would be properly designed for *in vivo* validation experiments (Fig. 5).

Also shown in Fig. 3a, is a linear fit to the data (straight line). A linear response to sweat volume is attractive from a measurement perspective, but was unexpected from a hydrogel swelling perspective. Fluid addition directly translates to increased hydrogel volume ( $V$ ), but if the hydrogel were to uniformly swell in all directions, hydrogel volume ( $V$ ) would translate to increased visible area ( $A$ ) for the hydrogel with a mathematical  $2/3^{\text{rd}}$  root dependence (non-linear). We initially speculated that friction in the patch could hinder lateral spreading of the hydrogel, but even when testing freely floating hydrogels we observe that they increase in thickness at a rate faster than they increase in horizontal dimension. Regardless, the purpose of Fig. 3a is for calibration, and as will be seen in other data (Fig. 3b, Fig. 5e) a linear response of area to sweat volume was repeatable, and therefore useful.

Fig. 3b includes similar calibration data, but for the continuous 'smart watch' mode of Fig. 1d. In this mode, a subset of the total hydrogel grid area would be measured using a simple LED and photodiode configuration similar to that already commonly deployed in smart-watches and other optical-mode wearables.<sup>21</sup> Almost an identical calibration behaviour is found between the Fig. 3a and 3b, suggesting that other alternate geometrical designs of the hydrogel are also feasible. The white area plotted in Fig. 3b is easily translatable to percent reflection measured by an optical wearable device, and importantly, the because of device intrinsically has zero-sweat calibration, change in reflection is all that needs to be measured (not absolute quantified reflection). With the blue-colourant utilized in this work, the

gels will increase in optical transmission as they swell. If this presents any issues in application, it can easily be mitigated by establishing a simple calibration curve, or by using a higher optical density colourant like carbon-black.

The data in Fig. 3b and 3a should theoretically respond to sweat with a similar trend, and because the data confirms a similar linear trend, only the smart-phone mode approach (Fig. 1c, Fig. 3a) was further *in vivo* validated. Simply, additionally *in-vivo* validating the smart-watch mode would not provide any insights beyond those gained for the smart-phone mode.

Before *in vivo* validation was to be explored, one more *in vitro* experiment was performed. Although custom-made hydrogels should perform over a wide pH and salinity range, that assumption was tested over non-pathological ranges for, sweat pH (4 to 9)<sup>22</sup> and salinity (10 to 100 mM NaCl)<sup>23</sup>. The data of Fig. 4 confirms robust and repeatable performance of the hydrogels with varying pH and salinity.

## ***In vivo* Patch Design and Results**

The design for the *in vivo* patch validation also utilized the 85  $\mu$ m thick hydrogel hexagons characterized in Figs. 3 and 4. The complete patch design of Fig. 5a also involves several additional features that are not captured in the simple diagram of Fig. 1a. To ensure a well-defined sweat collection area under the patch (see Requirements and Challenges section), a hydrogel/rayon seal ring was used to prevent collection of sweat from outside the defined collection area (Fig. 5a). The hydrogel used in the seal ring was also 85  $\mu$ m thick, was 1.5 mm wide, with a perimeter length of 6.27 cm.

The *in vivo* validation was performed using aerobic cycling of a subject in a room held at 25 degrees C (Fig. 5a). The exercise and measurement protocol is included with the online supplementary materials for this paper. Patches were placed on both the left and right biceps and forearms of a subject (labeled as Left bicep, Left forearm, Right bicep, Right forearm). The *in vivo* data is shown in Fig. 5a, and includes a

data set for 'actual sweat rate' which was measured gravimetrically<sup>13</sup> near the patch. The measured data is created using the calibration curve from Fig. 3a, and is fairly consistent for both arms. The measured data is somewhat initially consistently below that of the actual measured sweat rate. This lower initial measurement could be due to the initial volume capacity of the skin surface and the Rayon, which must be partially filled before sweat can reach the hydrogel hexagons. Overall, the *in vivo* data provides results that are expected based on the performance predicted by the *in vitro* data.

## Remaining Issues and Discussion

In this work, the primary goal was to demonstrate the patch design, operation, and initial *in vivo* validation. With this goal now complete, remaining issues and future work should be briefly discussed. Firstly, as speculated in the Requirements and Challenges sub-section, an ideal use of the patches discussed herein could be as follows. A user would measure nude bodyweight, then multiple patches applied across the body, then sweating would be generated by thermal or exercise methods. After the sweating, the multiple patches would be measured by smart-phone photos (Fig. 1c) and image analysis, along with a final recording of nude body weight. Then calibration curves would be generated for the individual. Once an individual was calibrated, they could then transition to 'smart watch mode' using one or fewer patches along with continuous optical read-out devices (Fig. 1d). This need for multi-body-site calibration of a sweat-rate sensing patch has been recently demonstrated by the Javi research group.<sup>16</sup> It could also be that a user enters a digital log-book of bodily sweat volume loss (nude-weight before and after) over time with repeated use of a single 'smart watch' device (Fig. 1d), and the device self-calibrates over time with improving predictive accuracy after each use.

To achieve all of this in practice, not only must patch robustness be further explored, but the predictive value must be determined for just how well localized sweat generation rate can be used to determine total bodily sweat volume loss. Furthermore, the adhesive area between the Rayon textile wicking layer and the hydrogel/Rayon leak ring has an area of ~2.78 cm<sup>2</sup> which, as noted in the Requirements and Challenges, should be reduced in area or eliminated completely to avoid unknown error the sweat collection area. Remaining work also includes design of automated image analysis software for 'smart-phone' mode, because in this work Image-J was manually utilized to measure hexagon area. Furthermore, in 'smart watch mode', any optical reflectance measurement should take into consideration confounding issues such as specular vs. diffuse reflection, motion induced changes in optical signal, etc. The patches could also benefit from a scaling feature as a dimensional control (see online ESI photo for example of such a patch with scaling feature). Regardless of these future improvements, the simplicity of the design used in this work offers significant promise to all these applications, because if the hydrogel receives sweat, the

hydrogel will swell in a predictable and easily measurable manner.

## Methods

### Materials

Samples of adhesive materials 3M9964, 3M4076 were obtained from 3M (Maplewood, MN). 99.0% Sodium chloride (NaCl), 99% poly (vin alcohol), 93% sodium hydroxide and 37% hydrochloric acid were obtained from Sigma-Aldrich (St. Louis, MO). Super absorbent polymer (ST-250\*) was obtained from Newstone (Tokyo, Japan). Blue colorant (450C) were obtained from Cabot (Alpharetta, GA). Plastic sheets (30 cm x 30 cm, 0.5 mm thick) were obtained from Grafix (Maple Heights, OH). The Rayon textile was obtained from WPT Nonwovens (Beaver Dam, KY). Ultrapure water (resistivity: 18.2 MΩ cm) was obtained from an EMD Millipore Direct-Q® 3 UV water purification system (Darmstadt, Germany).

### Hydrogel Fabrication

Super absorbent gel was prepared with a customized process provided by Eccrine Systems Inc. The hydrogel was made by thermal cross-linking of poly (sodium prop-2-enoate) using poly (vinyl alcohol) hydrogels (PAA-PVA hydrogels). 10 g of the resulting super absorbent polymer was added to 400 mL of water with stirring for 1 hour at 60 °C. The mixture was dried in oven at 60 °C overnight and lost ~200 g of water creating a gel-like material. 10% of PVOH was added to the super absorbent gel along with 0.5 mL of the Cabot 450C blue colourant. This mixture was then doctor-blade coated onto a plastic sheet and dried at 40 °C overnight. The resulting hydrogel film was then stored along with a desiccant to prevent water absorption during storage. The hydrogel films were then laser cut into hexagons using a Desktop laser Platforms (VLS3.50, Scottsdale, AZ) at settings of 25% of power and 100% of speed.

### Patch Fabrication

Simple layer-by-layer lamination of the device was utilized. An AutoCAD file of the assembly layers, a schedule detailing the function and preparation of each layer are provided with the ESI Tables. Detailed fabrication steps are provided in ESI Operations.

### In Vitro Testing

The photographs of the characterization were taken by using a Single Lens Reflex Camera from Canon U.S.A., Inc (Melville, NY). The hexagon area change was co-ordinately analyzed by using two software programs, Photoshop (available at adobe.com) for isolating the colour and Image-J (available at imagej.net) for calculating the total area of all the hydrogel hexagons in a patch.

Image-J codes for smart-phone mode operation are provided with the online ESI material.

**In vivo Testing**

Human subjects testing was performed by Eccrine Systems Inc. under their own approved human-subjects testing protocol for sweat rate measurement, and the de-identified data shared with the University of Cincinnati for use in this manuscript. The patch photographs were taken by an iPhone 7 Plus smartphone by using the original camera App. The exercise and measurement protocol is included with the online supplementary materials for this paper.

**Conflicts of interest**

Corresponding author Jason Heikenfeld has an equity interest in Eccrine Systems, Inc., a company that may potentially benefit from the research results, and also serves on the company's Board. The terms of this arrangement have been reviewed and approved by the University of Cincinnati in accordance with its conflict of interest policies.

**Acknowledgements**

The authors acknowledge partial support from the National Science Foundation EPDT Award #1608275, and the Ohio Federal Research Network (PO FY16-049; WSARC-1077-700). Both Feijun Zhao and Professor Mathias Bonmarin were visiting the University of Cincinnati as guest researchers during the work performed in this paper. This research was supported in part by the Study Abroad Program for Graduate Student of GUET (GDYX2018003), Innovation Project of Guangxi Graduate Education (YCBZ2019052), and GUET Excellent Graduate Thesis Program (16YJPYBS03). Professor Mathias Bonmarin was supported by a Fulbright visiting scholarship.

**References**

- J. Heikenfeld, *Electroanalysis*, 2016, **28**, 1242–1249.
- J. Heikenfeld, A. Jajack, B. Feldman, S. W. Granger, S. Gaitonde, G. Begtrup and B. A. Katchman, *Nat. Biotechnol.*, 2019, **37**, 407–419.
- A. Hauke, P. Simmers, Y. R. Ojha, B. D. Cameron, R. Ballweg, T. Zhang, N. Twine, M. Brothers, E. Gomez and J. Heikenfeld, *Lab Chip*, 2018, **18**, 3750–3759.
- M. Bariya, H. Y. Y. Nyein and A. Javey, *Nat. Electron.*, 2018, **1**, 160–171.
- T. Kaya, G. Liu, J. Ho, K. Yelamarthi, K. Miller, J. Edwards and A. Stannard, *Electroanalysis*, 2019, **31**, 411–421.
- Z. Sonner, E. Wilder, J. Heikenfeld, G. Kasting, F. Beyette, D. Swaile, F. Sherman, J. Joyce, J. Hagen, N. Kelley-Loughnane and R. Naik, *Biomicrofluidics*, 2015, **9**, 031301.
- D. P. Rose, M. E. Ratterman, D. K. Griffin, L. Hou, N. Kelley-Loughnane, R. R. Naik, J. A. Hagen, I. Papautsky and J. C. Heikenfeld, *IEEE Trans. Biomed. Eng.*, 2015, **62**, 1457–1465.
- M. J. Buono, C. S. White and K. P. Connolly, *J. Dermatol. Sci.*, 1992, **4**, 33–37.
- J. B. Mitchell and K. W. Voss, *Med. Sci. Sports Exerc.*, 1991, **23**, 314–319.
- P. D. Neuffer, A. J. Young and M. N. Sawka, *Eur. J. Appl. Physiol. Occup. Physiol.*, 1989, **58**, 433–439.
- B. P. McDermott, S. A. Anderson, L. E. Armstrong, D. J. Casa, S. N. Cheuvront, L. Cooper, W. Larry Kenney, F. G. O'Connor and W. O. Roberts, *J. Athl. Train.*, 2017, **52**, 877–895.
- L. Hou, J. Hagen, X. Wang, I. Papautsky, R. Naik, N. Kelley-Loughnane and J. Heikenfeld, *Lab Chip*, 2013, **13**, 1868–1875.
- P. Simmers, S. K. Li, G. Kasting and J. Heikenfeld, *J. Dermatol. Sci.*, 2018, **89**, 40–51.
- A. Koh, D. Kang, Y. Xue, S. Lee, R. M. Pielak, J. Kim, T. Hwang, S. Min, A. Banks, P. Bastien, M. C. Manco, L. Wang, K. R. Ammann, K. I. Jang, P. Won, S. Han, R. Ghaffari, U. Paik, M. J. Slepian, G. Balooch, Y. Huang and J. A. Rogers, *Sci. Transl. Med.*, 2016, **8**, 366ra165.
- H. Y. Y. Nyein, M. Bariya, L. Kivimäki, S. Uusitalo, T. S. Liaw, E. Jansson, C. H. Ahn, J. A. Hangasky, J. Zhao, Y. Lin, T. Happonen, M. Chao, C. Liedert, Y. Zhao, L.-C. Tai, J. Hiltunen and A. Javey, *Sci. Adv.*, 2019, **5**, eaaw9906.
- Z. Yuan, L. Hou, M. Bariya, H. Y. Y. Nyein, L.-C. Tai, W. Ji, L. Li and A. Javey, *Lab Chip*, 2019, **19**, 3179–3189.
- J. Francis, I. Stamper, J. Heikenfeld and E. F. Gomez, *Lab Chip*, 2019, **19**, 178–185.
- W. Gao, S. Emaminejad, H. Y. Y. Nyein, S. Challa, K. Chen, A. Peck, H. M. Fahad, H. Ota, H. Shiraki, D. Kiriya, D. H. Lien, G. A. Brooks, R. W. Davis and A. Javey, *Nature*, 2016, **529**, 509–514.
- N. B. Twine, R. M. Norton, M. C. Brothers, A. Hauke, E. F. Gomez and J. Heikenfeld, *Lab Chip*, 2018, **18**, 2816–2825.
- X. J. Liu, H. Q. Li, B. Y. Zhang, Y. J. Wang, X. Y. Ren, S. Guan and G. H. Gao, *RSC Adv.*, 2016, **6**, 4850–4857.
- J. Heikenfeld, A. Jajack, J. Rogers, P. Gutruf, L. Tian, T. Pan, R. Li, M. Khine, J. Kim, J. Wang and J. Kim, *Lab Chip*, 2018, **18**, 217–248.
- J. Fei, Z. Zhang, L. Zhong and L. Gu, *J. Appl. Polym. Sci.*, 2002, **85**, 2423–2430.
- S. M. M. Quintero, R. V. Ponce F, M. Cremona, A. L. C. Triques, A. R. D'Almeida and A. M. B. Braga, *Polymer*, 2010, **51**, 953–958.

Presented is ultra-simple wearable local sweat volume monitoring patch based on swellable hydrogels.

